

SYNLIPMAE: CONTRASTIVE MASKED PRETRAINING FOR AUDIO-VISUAL TALKING-FACE REPRESENTATIONS

Zeyu Ling^{1,*} Xiaodong Gu^{2,*} Jiangnan Tang² Changqing Zou^{1,†}

¹ State Key Laboratory of CAD&CG, Zhejiang University ² ByteDance
 {zeyuling, changqing.zou}@zju.edu.cn
 vactor1994@gmail.com, jiangnantang@outlook.com

ABSTRACT

We introduce SyncLipMAE, a self-supervised pretraining framework for talking-face video that learns synchronization-aware and transferable facial dynamics from unlabeled audio-visual streams. Our approach couples masked visual modeling with cross-modal contrastive alignment and employs three per-frame prompt tokens that explicitly encode the essential factors of a talking-face frame—identity, vocal motion (speech-synchronized facial dynamics), and ambient motion (audio-agnostic movements such as blinks and head pose). The contrastive objective uses time-aligned vocal-motion and audio tokens as positives and misaligned pairs as negatives, driving both modalities into a shared embedding space and yielding token-level audio-visual stream synchronization. After pretraining, the aligned audio tokens together with the visual prompt tokens (identity, vocal motion, ambient motion) form a unified interface for four disparate downstream settings: (i) audio-visual stream synchronization; (ii) facial emotion and head/face action recognition; (iii) visual speech recognition; and (iv) visual dubbing, for which we, for the first time, enable indistinguishable audio- or video-driven control within a single model. Across four task families that require distinct capabilities, SyncLipMAE achieves state-of-the-art results, underscoring the effectiveness of synchronization-aware, factorized self-supervised pretraining.

1 INTRODUCTION

Talking-face video underpins human-computer interaction, accessibility, content creation, and post-production. Practical systems must jointly reason about linguistic content, audio-visual timing, video editing to match a target speech track or reference motion, and facial expressions/actions. Classic synchronisation pipelines such as SyncNet and subsequent Transformer-based variants (e.g., VocaLiST) focus on detecting in-/out-of-sync pairs or removing stream lags, while recent audio-visual pretraining methods (e.g., AV-HuBERT) have shown strong transfer to lip reading and AV-ASR. Yet, these advances do not directly yield a *token-level*, stream-synchronised representation that cleanly separates identity, speech-synchronised mouth motion, and other facial dynamics—capabilities that are essential for both analysis and controllable generation.

Most prior work tackles one facet at a time. Visual or video masked modeling (MAE/VideoMAE) excels at reconstruction but is modality-specific and does not enforce audio-visual alignment; contrastive AV learning improves correspondence but is typically framed as binary sync classification rather than a shared token space; and dubbing systems (e.g., Wav2Lip, LatentSync, MuseTalk) optimise for generation quality and lip accuracy but are not designed to provide a unified interface that can be driven interchangeably by audio or reference motion within a single model. As a result, existing solutions often rely on wider temporal windows or task-specific heads, and they lack a factorised, alignment-aware representation that transfers seamlessly across synchronisation, understanding, and dubbing.

We introduce SyncLipMAE, a self-supervised pretraining framework tailored to talking-face video. SyncLipMAE learns three per-frame prompt tokens—**identity**, **vocal motion** (speech-synchronised

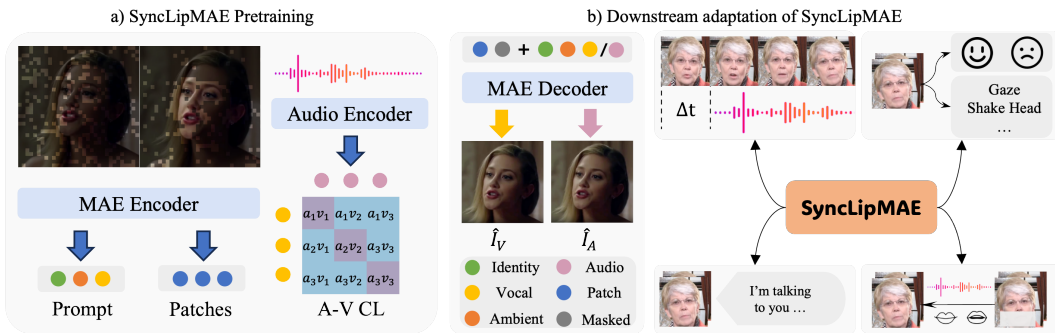


Figure 1: Panel (a) schematically illustrates the core components of SyncLipMAE and the computational pipeline used during pretraining, while panel (b) shows its adaptation to downstream tasks.

dynamics), and **ambient motion** (audio-agnostic movements)—and couples masked visual reconstruction with a cross-modal contrastive objective that aligns vocal-motion tokens to temporally matched audio tokens in a shared embedding space. A two-view masking strategy (uniform vs. face-preserving) sources patch context and factor prompts, and a simple identity-shuffle regulariser further purifies the identity token. Decoding is performed in two passes per frame (video- and audio-conditioned) with shared weights, which provides symmetric supervision that tightens audio–visual stream synchronization at the token level. This factorised, aligned interface directly supports diverse downstream uses without task-specific architecture changes.

Beyond analysis, SyncLipMAE enables *unified* visual dubbing: using a WanVACE-style DiT backbone for masked video inpainting, we inject either aligned audio tokens or vocal-motion tokens *after* patch embedding via a lightweight AudioPack, so the same model admits no-difference audio- or video-driven control. This preserves identity and pose while re-synchronising the mouth region, and it naturally benefits from the shared token space learned during pretraining.

Contributions. (i) We propose a synchronization-aware, factorised pretraining scheme that yields three prompt tokens (identity, vocal motion, ambient motion) and a shared audio–visual token space. (ii) We introduce a two-view masking design and identity-shuffle regularisation tailored to talking faces. (iii) We show a unified dubbing interface that *for the first time* enables no-difference audio- or video-driven control within a single model by injecting aligned control tokens into a WanVACE backbone. (iv) We demonstrate state-of-the-art performance across four distinct tasks—audio–visual stream synchronization, facial expression/action understanding, visual speech recognition, and visual dubbing—highlighting the effectiveness and generality of the approach.

2 RELATED WORK

Audio–visual synchronisation and correspondence. A long line of work formulates A/V learning as correspondence or temporal alignment. Arandjelovic & Zisserman (2017) learns generic audio–visual correspondence from unlabelled video, while Morgado et al. (2020) casts synchronisation as in-time vs. out-of-time discrimination within the same clip. For faces, Chung & Zisserman (2016) introduces a two-stream embedding for lip–audio alignment and lag estimation; recent transformers such as Kadandale et al. (2022) improve robustness across speech/singing with longer-range context.

Masked modelling and contrastive learning at scale. Contrastive pretraining aligns paired modalities at scale (e.g., CLIP Radford et al. (2021)), while masked autoencoders (MAE He et al. (2022)/VideoMAE Tong et al. (2022)) show that reconstructing heavily masked inputs yields strong visual/video representations. These paradigms are complementary and now standard building blocks for multimodal pretraining.

Facial video representation pretraining. Closer to our setting, MARLIN Cai et al. (2023) applies masked autoencoding to facial videos, using facial-region-guided masking to learn a universal face encoder transferable to expression recognition, deepfake detection, etc. Subsequent variants adapt

Table 1: Lip synchronisation on **Hallo3**. Higher is better for Acc and R-Precision; lower is better for Offset.

Method	K = 1		K = 5		K = 15		R-precision (32)		
	Acc \uparrow (%)	Offset \downarrow	Acc \uparrow (%)	Offset \downarrow	Acc \uparrow (%)	Offset \downarrow	Top1 \uparrow	Top2 \uparrow	Top3 \uparrow
SyncNet -5	20.37	5.04	24.18	4.03	30.03	3.02	7.47	12.77	17.72
VocaLiST -5	21.85	4.34	24.56	3.63	28.82	2.98	8.80	15.08	19.86
StableSyncNet -16	27.95	2.78	28.60	2.72	31.66	2.72	14.40	25.65	34.52
SyncLipMAE -1 (ours)	52.53	2.66	68.41	1.73	82.27	0.93	40.18	61.48	73.49

MAE-style pretraining to dynamic facial expression recognition under limited labels Sun et al. (2023). While these works focus on reconstruction-only objectives within the facial domain, we couple MAE with audio–visual contrast to align speech-driven dynamics, and structure the representation to separate identity and motion factors.

Visual speech recognition and audio–visual ASR. From early end-to-end lipreading (LipNet) to large-scale self-supervised A/V pretraining (AV-HuBERT) and automated VSR/AVSR recipe design (Auto-AVSR Ma et al. (2023)), results consistently show that robust visual streams improve recognition and benefit from pretraining on unlabelled A/V data.

Talking-face generation and lip-sync synthesis. Audio-driven talking-head synthesis has progressed from GAN-based pipelines with explicit sync critics (e.g., Wav2Lip Prajwal et al. (2020)) to diffusion in latent/image space (e.g., LatentSync Li et al. (2024)) and efficient diffusion heads (MuseTalk Zhang et al. (2024)). In parallel, foundation video generators and unified conditional DiT Peebles & Xie (2023) frameworks (WAN Wan et al. (2025); VACE Jiang et al. (2025)) provide scalable backbones and conditioning interfaces (Video Condition Unit, context adapters) for editing or T2V, which our dubbing setup leverages.

3 SYNCLIPMAE: PRETRAINING OBJECTIVE AND ARCHITECTURE

3.1 OVERVIEW AND DESIGN GOALS

SyncLipMAE aims to learn synchronization-aware talking-face representations from unlabeled audio–visual streams. As illustrated in figure 1(a), our approach couples MAE-style masked image/video modeling on the visual stream with a CLIP-style cross-modal contrastive alignment that treats time-aligned *vocal-motion* and *audio* tokens as positives and temporally misaligned pairs as negatives, driving both modalities into a shared embedding space and yielding token-level audio–visual stream synchronization (§3.3). Per frame, a ViT-based encoder exposes three prompt tokens that explicitly encode the essential factors of a talking-face frame—identity \mathbf{z}^{id} , vocal motion \mathbf{z}^{voc} , and ambient motion \mathbf{z}^{amb} —and the decoder reconstructs frames via cross-attention conditioned on these prompts.

Inputs and Notation. Let $\mathbf{x}_{1:T} \in \mathbb{R}^{T \times C \times H \times W}$ be video frames and $\mathbf{a} \in \mathbb{R}^N$ mono audio at sampling rate f_s . Each frame is patchified into N_p patches and embedded to D -dimensional tokens. For MAE-style masking, denote by $\mathcal{V}_t \subset \{1, \dots, N_p\}$ the indices of visible patches at time t and by \mathcal{M}_t the masked ones, with $|\mathcal{V}_t| = N_{\text{vis}}$ and $\mathcal{V}_t \cup \mathcal{M}_t = \{1, \dots, N_p\}$. The per-frame visible patch tokens are $\mathbf{P}_t^{\text{vis}} \in \mathbb{R}^{N_{\text{vis}} \times D}$. Let $\mathbf{e}^{\text{mask}} \in \mathbb{R}^D$ be a learnable mask token; a restoration operator places $\mathbf{P}_t^{\text{vis}}$ and copies of \mathbf{e}^{mask} at indices \mathcal{M}_t to form a length- N_p sequence for decoding. Per frame, the encoder also outputs three prompt tokens, $\mathbf{z}_t^{\text{id}}, \mathbf{z}_t^{\text{amb}}, \mathbf{z}_t^{\text{voc}} \in \mathbb{R}^D$. For audio, we employ a pretrained speech encoder with L layers that is kept frozen during pretraining; let $\{\mathbf{H}^{(\ell)}\}_{\ell=1}^L$ denote the hidden-state sequences from all layers. To obtain frame-wise alignment with the video, we resample the input waveform so that the encoder emits T tokens per utterance (one token per video frame) at every layer, yielding $\mathbf{A}^{(\ell)} = \{\mathbf{a}_t^{(\ell)}\}_{t=1}^T$.

Table 2: Lip synchronisation on VFHQ.

Method	K = 1		K = 5		K = 15		R-precision (32)		
	Acc \uparrow (%)	Offset \downarrow	Acc \uparrow (%)	Offset \downarrow	Acc \uparrow (%)	Offset \downarrow	Top1 \uparrow	Top2 \uparrow	Top3 \uparrow
SyncNet-5	22.16	5.14	26.47	4.34	31.09	3.29	9.40	16.91	23.09
VocaLiST-5	21.76	5.14	24.34	4.57	29.23	3.62	10.18	16.56	21.98
StableSyncNet-16	32.40	3.17	33.06	3.07	35.43	2.90	23.54	37.65	46.77
SyncLipMAE -1 (ours)	38.58	3.80	48.95	3.06	61.78	2.16	35.52	52.98	63.37

3.2 MODEL DESIGN

Two-Bypass Face-Aware Masking. Each frame is processed by two masking *bypasses*, and the visual encoder is invoked twice per iteration to consume the corresponding visible patches. **Bypass 1 (Uniform)** applies a random uniform mask hiding 75% of patches, leaving the visible set $\mathcal{V}_t^{(1)}$ and visible patch tokens $\mathbf{P}_t^{\text{vis},(1)} \in \mathbb{R}^{N_{\text{vis}} \times D}$. We use the *identity* prompt \mathbf{z}_t^{id} from this pass together with these visible patch tokens for decoding; the *vocal/ambient* prompts from this pass are ignored. **Bypass 2 (Face-Preserving)** also masks 75% of patches but retains facial regions with higher keep probability, forming $\mathcal{V}_t^{(2)}$. To suppress appearance leakage while preserving motion cues, we apply color/brightness/saturation perturbations on this view. We use the *vocal-motion* and *ambient-motion* prompts $\mathbf{z}_t^{\text{voc}}, \mathbf{z}_t^{\text{amb}}$ from this pass for decoding, while its visible patch tokens and identity prompt are ignored. In both passes the encoder consumes only visible patches. Before decoding, a learnable mask token is inserted at indices $\mathcal{M}_t^{(1)}$ (the complement of $\mathcal{V}_t^{(1)}$) to restore a length- N_p sequence per frame, consistent with MAE.

Visual Encoder and Prompt Tokens. A ViT-style encoder applied to the visible patches outputs per-frame patch tokens (from Bypass 1) and three prompt tokens

$$\mathbf{Z}_t^{\text{prompt}} = [\mathbf{z}_t^{\text{id}}, \mathbf{z}_t^{\text{amb}}, \mathbf{z}_t^{\text{voc}}] \in \mathbb{R}^{3 \times D},$$

where \mathbf{z}_t^{id} is taken from Bypass 1 and $\mathbf{z}_t^{\text{voc}}, \mathbf{z}_t^{\text{amb}}$ from Bypass 2 as defined above.

Identity-Consistent Prompt Shuffling. Within a mini-batch, to promote motion-invariant identity embeddings, we randomly swap \mathbf{z}^{id} among frames that share the same subject identity but exhibit different facial motions, weakening incidental coupling between identity prompts and short-term dynamics.

Audio Features and Adapter. A pretrained L -layer speech encoder (kept frozen) produces per-layer hidden sequences; we resample the input waveform so that each layer emits T tokens (one per video frame), yielding aligned streams $\{\mathbf{a}_t^{(\ell)}\}_{t=1}^T$. To preserve both low-level acoustic detail and higher-level linguistic cues, we concatenate the aligned per-layer tokens along the feature dimension at each time step,

$$\tilde{\mathbf{a}}_t = [\mathbf{a}_t^{(1)} \parallel \dots \parallel \mathbf{a}_t^{(L)}],$$

and pass them through an audio adapter that projects to the shared width D , producing $\mathbf{A}_t \in \mathbb{R}^D$. This design mitigates the bias of top encoder layers toward semantic content induced by ASR pretraining while retaining waveform-proximal information from earlier layers.

Decoder with Prompt Cross-Attention. We use an MAE-style decoder with N_{dec} Transformer blocks. Its input at each frame is the restored token sequence formed by encoded visible patches from Bypass 1 plus mask tokens (with positional embeddings). Each block first applies self-attention over this full sequence (visible patches + mask tokens), and then cross-attends to the prompt tokens—identity, ambient, and a conditioning token \mathbf{c}_t . We perform two decoding passes per frame that share decoder weights: (i) a video-driven pass with $\mathbf{c}_t = \mathbf{z}_t^{\text{voc}}$ producing $\hat{\mathbf{x}}_t^{\text{voc}}$, and (ii) an audio-driven pass with $\mathbf{c}_t = \mathbf{A}_t$ producing $\hat{\mathbf{x}}_t^{\text{aud}}$. Both passes reconstruct the same target frame \mathbf{x}_t , providing symmetric supervision that encourages the vocal-motion and audio tokens to encode consistent, alignable information. A linear head maps decoded tokens back to pixels.

Table 3: CelebV-HQ emotion and action classification. Higher is better (Accuracy/AUC).

Method	Frames	Emotion		Action	
		Accuracy \uparrow	AUC \uparrow	Accuracy \uparrow	AUC \uparrow
VideoMAE	1×16	68.63	60.32	93.97	84.31
VideoMAE	5×16	68.63	66.60	94.54	86.01
MARLIN	1×16	66.67	58.15	94.69	82.26
MARLIN	5×16	69.61	64.98	94.86	83.90
SyncLipMAE (ours)	16	76.47	73.94	95.06	86.45
SyncLipMAE (ours)	80	77.45	78.33	95.11	86.69

3.3 PRETRAINING OBJECTIVES

Pixel-Space Reconstruction (MSE). We minimize per-frame mean squared error for the two decoding passes (video-driven and audio-driven; see §3.2):

$$\mathcal{L}_{\text{pix}}^{\text{voc}} = \frac{1}{T} \sum_{t=1}^T \|\hat{\mathbf{x}}_t^{\text{voc}} - \mathbf{x}_t\|_2^2, \quad \mathcal{L}_{\text{pix}}^{\text{aud}} = \frac{1}{T} \sum_{t=1}^T \|\hat{\mathbf{x}}_t^{\text{aud}} - \mathbf{x}_t\|_2^2.$$

Audio–Vocal Contrastive Alignment. Unlike prior audio–visual synchronisation systems that cast the task as in-/out-of-sync *binary* classification or as *pairwise* contrastive matching, we align per-frame audio tokens \mathbf{A}_t with vocal-motion tokens $\mathbf{v}_s = \mathbf{z}_s^{\text{voc}}$ using a CLIP-style symmetric InfoNCE. Let $p_{t \rightarrow s} = \frac{\exp(\langle \mathbf{A}_t, \mathbf{v}_s \rangle / \tau)}{\sum_{u=1}^T \exp(\langle \mathbf{A}_t, \mathbf{v}_u \rangle / \tau)}$ be the softmax over vocal candidates for audio index t , and P_t the positive set (aligned index and optional neighbors within $\pm k$, expanded by an audio self-similarity threshold). The loss is

$$\mathcal{L}_{\text{CL}} = -\frac{1}{2T} \sum_{t=1}^T \left[\log \sum_{s \in P_t} p_{t \rightarrow s} + \log \sum_{s \in P_t} p_{s \rightarrow t} \right],$$

with temperature τ . This preserves CLIP-style bidirectional alignment while allowing multiple positives per anchor.

Cross-Covariance Decorrelation. To reduce leakage across factor-specific embeddings, we penalize cross-covariance between centered tokens. For $\mathcal{P} = \{\text{id}, \text{amb}, \text{voc}\}$:

$$\mathcal{L}_{\text{cov}} = \frac{1}{D^2} \sum_{\{p,q\} \subset \mathcal{P}} \|\text{Cov}(\mathbf{z}^p, \mathbf{z}^q)\|_F^2,$$

where covariance is computed after centering along the batch/time axis.

Total Objective. The overall loss is

$$\mathcal{L} = \lambda_{\text{pix}} (\mathcal{L}_{\text{pix}}^{\text{voc}} + \mathcal{L}_{\text{pix}}^{\text{aud}}) + \lambda_{\text{CL}} \mathcal{L}_{\text{CL}} + \lambda_{\text{cov}} \mathcal{L}_{\text{cov}}.$$

4 DOWNSTREAM ADAPTATION

We apply SyncLipMAE to four tasks: **(i) audio–visual stream synchronization** — infer frame-level lag and synchrony by comparing aligned audio tokens \mathbf{A}_t with vocal-motion tokens $\mathbf{z}_t^{\text{voc}}$; **(ii) facial understanding** — infer emotion and head/face actions from the vocal- and ambient-motion tokens; **(iii) visual speech recognition (VSR)** — infer text from the vocal-motion tokens; **(iv) visual dubbing** — edit a source face video to match target speech or a reference motion, supporting audio- or video-driven control within a single model.

Table 4: Video dubbing on **VFHQ** and **Hallo3**. **A-** denotes audio-driven control; **V-** denotes video-driven control. Higher is better for $\text{Sync}_{\text{conf}}$; lower is better for FID/FVD.

Method	VFHQ			Hallo3		
	$\text{Sync}_{\text{conf}} \uparrow$	FID \downarrow	FVD \downarrow	$\text{Sync}_{\text{conf}} \uparrow$	FID \downarrow	FVD \downarrow
MuseTalk Zhang et al. (2024)	0.6820	24.44	175.16	0.6904	13.80	86.46
LatentSync-1.5 Li et al. (2024)	0.7681	17.92	131.04	0.7725	10.59	78.89
A-SyncLipMAE (ours)	0.7830	16.46	100.44	0.8027	10.04	74.01
V-SyncLipMAE (ours)	–	17.22	109.91	–	10.82	77.57

4.1 AUDIO-VISUAL SYNCHRONISATION

We estimate audio–video lag directly in the pretrained shared space without any extra head or training. Given per-frame audio tokens \mathbf{A}_t and vocal-motion tokens $\mathbf{z}_s^{\text{voc}}$, compute frame-wise cosine similarity

$$s(t, s) = \langle \mathbf{A}_t, \mathbf{z}_s^{\text{voc}} \rangle,$$

and aggregate along temporal offsets

$$S(\Delta) = \frac{1}{T-|\Delta|} \sum_{t=1}^{T-|\Delta|} s(t, t+\Delta), \quad \hat{\Delta} = \arg \max_{\Delta \in [-\Delta_{\text{max}}, \Delta_{\text{max}}]} S(\Delta).$$

The in-sync score is $S(0)$ and the estimated lag is $\hat{\Delta}$. All computations use the frozen tokens from pretraining; no correspondence MLP or additional supervision is introduced.

4.2 FACIAL UNDERSTANDING: EMOTION AND ACTION

We use SyncLipMAE’s motion factors per frame and keep the prediction head minimal. For each frame t , we form a motion descriptor by averaging the two factors, $\mathbf{u}_t = \frac{1}{2}(\mathbf{z}_t^{\text{voc}} + \mathbf{z}_t^{\text{amb}})$, and apply a single linear classifier to obtain frame-level logits. Video-level logits are the mean of frame-level logits over the sampled frames; the final prediction is the softmax over the aggregated logits. This setup probes whether the representation cleanly separates speech-synchronized orofacial motion from audio-agnostic dynamics (e.g., blinks, head pose) while keeping the adaptation lightweight; datasets such as CelebV-HQ provide the emotion/action labels used in this setting.

4.3 LIP READING (VSR)

We use a visual-only sequence-to-sequence head on top of SyncLipMAE’s vocal-motion tokens. Let $\mathbf{V} = \{\mathbf{z}_t^{\text{voc}}\}_{t=1}^{T'}$ be the input to a Conformer encoder, yielding hidden states $\mathbf{H} = \{\mathbf{h}_t\}_{t=1}^{T'}$. A Transformer decoder autoregressively predicts subword units with cross-attention to \mathbf{H} .

Losses. Let the target token sequence be $Y = \{y_u\}_{u=1}^U$ over vocabulary Σ (blank \emptyset for CTC). The CTC branch defines

$$P_{\text{CTC}}(Y | \mathbf{H}) = \sum_{\pi \in \mathcal{B}^{-1}(Y)} \prod_{t=1}^{T'} p_{\text{ctc}}(\pi_t | \mathbf{h}_t), \quad \mathcal{L}_{\text{CTC}} = -\log P_{\text{CTC}}(Y | \mathbf{H}),$$

where \mathcal{B} collapses repeats and removes blanks. The decoder branch is trained with teacher forcing:

$$\mathcal{L}_{\text{DEC}} = -\sum_{u=1}^U \log p_{\text{dec}}(y_u | y_{<u}, \mathbf{H}).$$

The total objective is the standard hybrid form

$$\mathcal{L}_{\text{VSR}} = \lambda_{\text{CTC}} \mathcal{L}_{\text{CTC}} + (1 - \lambda_{\text{CTC}}) \mathcal{L}_{\text{DEC}},$$

with a tunable weight $\lambda_{\text{CTC}} \in (0, 1)$.

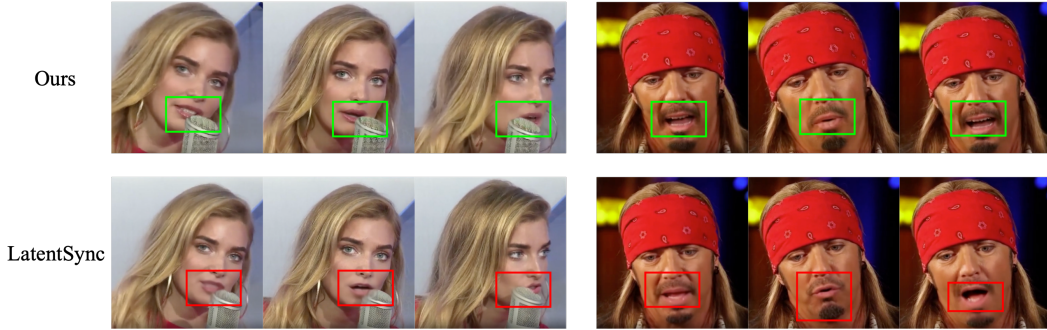


Figure 2: Qualitative visual comparison: LatentSync vs. our approach.

4.4 VIDEO DUBBING

We cast dubbing as masked video inpainting on face crops within a VACE-style unified interface: task inputs (reference frames and a spatiotemporal mouth mask) are organized as a Video Condition Unit and processed by a Diffusion-Transformer backbone with Concept Decoupling and Context Adapters, following VACE. Concretely, we instantiate the pipeline on WanVACE and keep its architecture, losses, and training schedule unchanged. WanVACE natively accepts multiple reference images (1–3 in the public release), exposed as a comma-separated list, which we leverage for identity control.

Control injection. Inspired by audio-conditioned injection in recent avatar generation, we adopt a minimal *AudioPack* placed *after* the VACE patch-embedding stage and *before* the first DiT VACE block. Per-frame control tokens—either audio tokens \mathbf{A}_t produced by SyncLipMAE or reference vocal-motion tokens $\mathbf{z}_t^{\text{voc}}$ —are temporally encoded and projected to the DiT width, then *added* to the patch-embedded video token stream. No other WanVACE components are modified; switching \mathbf{A}_t vs. $\mathbf{z}_t^{\text{voc}}$ toggles audio-driven vs. video-driven control within the same model.

Long-form continuity via dual references. To support arbitrarily long, coherent dubbing, we provide two references: (i) an *identity* image (stable appearance prior), and (ii) the *last frame of the previous segment* (temporal bridge). During training we randomly drop the continuity reference with 10% probability, so the model can also initialize the *first* segment without a history frame.

Masking strategy. Following common lip-sync inpainting practice, we detect the facial region (chin to hairline) and mask the *lower half* as the editable area; to accommodate jaw excursions (post-edit lip motion often increases mouth opening), the mask is expanded slightly downward beyond the chin. This aligns with widely used lower-face inpainting setups in Wav2Lip-style and diffusion-based lip-sync systems.

5 EXPERIMENTS

Implementation details. *Backbones.* The visual encoder follows the Sapiens-0.3B configuration and is initialized from its pretrained weights; the decoder adopts the ViTMAE-B design with a cross-attention sublayer in every block to attend to the identity/ambient/vocal prompt tokens. The audio branch uses a pre-trained wav2vec 2.0 base encoder kept frozen during pretraining. *Pretraining.* SyncLipMAE is trained on 128 GPUs with a per-GPU batch size of 48 (global = 128×48) for 400k steps (15 days). *Video dubbing fine-tuning.* We initialize from WanVACE-1.3B, freeze Wan backbone blocks, and optimize only VACE blocks (0.7B trainable params). Training uses 128 GPUs, batch size 1 per GPU, for 30k steps (3 days). Each sample contains 17+1+1 frames: 17 target frames, one history frame (for temporal continuity), and one identity frame (appearance prior).

Table 5: Visual speech recognition on **VFHQ**, **Hallo3**, and **HDTF**. Lower is better (WER↓).

Method	WER↓		
	VFHQ	Hallo3	HDTF
AV-HuBERT Shi et al. (2022)	14.29	16.57	15.28
Auto-AVSR Ma et al. (2023)	8.13	6.23	5.91
SyncLipMAE	7.37	5.99	5.78

Pretraining data. We pretrain SyncLipMAE on a mixture of talking-face corpora: Hallo3 Cui et al. (2025), CelebV-HQ Zhu et al. (2022), CelebV-Text Yu et al. (2023), MEAD Wang et al. (2020), VFHQ Xie et al. (2022), HDTF Zhang et al. (2021) and RAVDESS Livingstone & Russo (2018). Unless specified, audio is mono 16 kHz and videos are 25 fps. We adopt the official train–val–test split when available; otherwise, we randomly sample 100 instances each for validation and testing, and use the remainder for training.

Audio–visual stream synchronization. We evaluate alignment under two complementary protocols that require no additional training: (i) *temporal lag detection* by sliding the offset between the audio token sequence $A = \{a_t\}_{t=1}^T$ and the visual token sequence $V = \{v_t\}_{t=1}^T$, and (ii) *audio→video token matching* reported as R-precision@ k .

Temporal lag detection. For a candidate lag $\tau \in \mathcal{T}$ (positive: video lags audio), define the average distance

$$D(\tau) = \frac{1}{T_\tau} \sum_{t=1}^{T_\tau} d(a_t, v_{t+\tau}),$$

with T_τ chosen so indices are valid and $d(\cdot, \cdot)$ a feature distance (e.g., cosine or ℓ_2). The estimated lag is

$$\hat{\tau} = \arg \min_{\tau \in \mathcal{T}} D(\tau).$$

Given ground-truth lag τ^* , we report

$$\text{Offset} = \frac{1}{N} \sum_{s=1}^N |\hat{\tau}^{(s)} - \tau^{(s)}| \quad \text{and} \quad \text{Acc}_{\pm K} = \frac{1}{N} \sum_{s=1}^N \mathbf{1}(|\hat{\tau}^{(s)} - \tau^{(s)}| \leq K).$$

Audio→Video token matching (R-precision@ k). We additionally report this retrieval-style metric because in segments with speaker silence or very small mouth motion the lag-based signal (Offset/Acc) can become weak or ambiguous, whereas a ranked retrieval test still probes cross-pair discriminability among distractors. Within a minibatch of size B , let $\{(a_i, v_i)\}_{i=1}^B$ be audio/visual token pairs and let \mathcal{P}_i be the candidate pool consisting of the true v_i plus non-matching video tokens (pool size fixed by the batch or a pre-defined sampler). Rank \mathcal{P}_i by distance to a_i and denote the rank of v_i by $\text{rank}_i(v_i)$ (1 is best). The retrieval metric is

$$\text{R-precision@}k = \frac{1}{B} \sum_{i=1}^B \mathbf{1}(\text{rank}_i(v_i) \leq k),$$

reported for small k (e.g., $k=1, 2, 3$) and fixed pool size (e.g., 32).

Results. Tab 1 and Tab 2 summarise results on Hallo3 and VFHQ. Across both datasets, SyncLipMAE consistently improves temporal alignment (higher $\text{Acc}_{\pm K}$, lower *Offset*) and cross-modal retrieval (higher R-precision@ k). Notably, these gains are achieved with single-frame visual conditioning ($n=1$), whereas baselines rely on wider temporal windows ($n=5$ or 16), indicating stronger per-frame audio–visual correspondence and reduced dependence on temporal aggregation.

Facial understanding (emotion & actions). We evaluate on **CelebV-HQ** Zhu et al. (2022) using the *emotion* and *action* attribute sets, reporting video-level Accuracy and AUC (higher is better). Emotion is treated as a *single-label*, 8-way classification task, whereas action is a *multi-label* problem over 35 categories (one-vs-rest scoring aggregated at the video level). To match common practice, clip-based baselines (e.g., VideoMAE/MARLIN) adopt the $a \times b$ protocol—uniformly sample a clips of b frames and average their predictions following Tong et al. (2022); frame-averaging models use n uniformly sampled frames and average per-frame predictions Korbar et al. (2019). All methods use a single linear classifier on frozen features. Let $\{\mathbf{x}_i\}_{i=1}^m$ be the sampled clips (or frames), $f(\cdot)$ the frozen encoder, and W the linear head; the video-level logits are

$$\bar{\ell}(V) = \frac{1}{m} \sum_{i=1}^m W f(\mathbf{x}_i), \quad \hat{y}(V) = \arg \max_k \text{softmax}_k(\bar{\ell}(V)),$$

with Accuracy/AUC computed from $\hat{y}(V)$ at the video level.

Results. Tab 3 summarises CelebV-HQ emotion and action. On emotion, SyncLipMAE clearly surpasses the best baseline with 16 frames and improves further at 80 frames, indicating benefits from longer temporal context. On action—where baselines are already strong—SyncLipMAE provides consistent but modest gains, with a slight boost when using 80 frames. Overall, SyncLipMAE delivers substantial improvements on emotion and steady gains on action.

Visual Speech Recognition (VSR) We evaluate SyncLipMAE on HDTF, VFHQ, and Hallo3, predicting text from silent videos. Following standard practice, accuracy is measured by Word Error Rate (WER), computed from word-level substitutions (S), deletions (D), and insertions (I) against the reference of length N :

$$\text{WER} = \frac{S + D + I}{N}.$$

Results. Tab 5 reports WER on VFHQ, Hallo3, and HDTF. The visual-only head built on SyncLipMAE’s tokens achieves the best WER on all three sets: 7.37 on VFHQ, 5.99 on Hallo3, and 5.78 on HDTF, improving over Auto-AVSR by absolute 0.76, 0.24, and 0.13 respectively, and substantially outperforming AV-HuBERT on each set. These gains indicate that SyncLipMAE’s pretraining yields visual motion features that transfer effectively to sentence-level lip reading under the standard hybrid CTC/attention recipe.

Video dubbing. We evaluate *video dubbing*—re-synchronising the mouth region of a source video to a target speech while preserving identity, pose, and expressions—using a WanVACE-based model that supports both audio- and video-driven conditioning via a lightweight vocal-cue injection (details in section 4.4). We report the metrics in Tab 4. $\text{Sync}_{\text{conf}}$ (identical to LSE-C) is computed with the *stable SyncNet* evaluator from LatentSync Li et al. (2024), replacing the commonly used vanilla SyncNet whose scores are less reliable in our experiments Prajwal et al. (2020). Following SyncNet Chung & Zisserman (2016), for each short sliding window we form an audio–video distance curve over temporal offsets $\Delta \in [-L, L]$:

$$d_t(\Delta) = \|\phi_a(a_{t:t+w-1}) - \phi_v(v_{t+\Delta:t+\Delta+w-1})\|_2,$$

and define the per-window confidence as the *median–minimum gap* on this curve,

$$\text{Conf}_t = \text{median}_{\Delta} d_t(\Delta) - \min_{\Delta} d_t(\Delta), \quad \text{Sync}_{\text{conf}} = \frac{1}{T} \sum_{t=1}^T \text{Conf}_t,$$

where larger values indicate a clearer minimum at the correct offset (stronger A/V synchrony) Chung & Zisserman (2016); Prajwal et al. (2020). **FID** measures per-frame perceptual quality via the Fréchet distance between Inception features of real vs. generated frames (lower is better) Heusel et al. (2017); **FVD** extends this to spatiotemporal video features to capture visual quality and temporal coherence jointly (lower is better) Unterthiner et al. (2018).

Results. Qualitatively (Fig. 2), SyncLipMAE preserves identity and fine lip details (e.g., teeth, beard) and is more robust to occlusions than LatentSync/MuseTalk. Quantitatively (Tab. 4), consistent with these observations, the audio-driven variant (**A-SyncLipMAE**) attains the best overall scores on synchrony ($\text{Sync}_{\text{conf}}$) and perceptual quality (FID/FVD) on both VFHQ and Hallo3. The video-driven variant (**V-SyncLipMAE**) closely matches the audio-driven performance and surpasses prior methods, indicating that the shared token space indeed aligns modalities and enables no-difference audio- or video-driven control within a single model.

Ablation Studies. We perform ablations on the key components of SyncLipMAE, examining: (i) whether to enable Two-Bypass Face-Aware Masking; (ii) the strategy for adapting audio features; and (iii) the inclusion of cross-attention in the decoder. Detailed results are provided in the Appendix.

6 CONCLUSION

We introduced SyncLipMAE, a self-supervised framework for talking-face video that couples masked visual reconstruction with contrastive audio–visual alignment and explicitly factorizes each frame into three prompt tokens—**identity**, **vocal motion**, and **ambient motion**. This design yields

synchronization-aware, disentangled features that transfer directly to diverse applications. Across four tasks—audio–visual stream synchronization, facial understanding, visual speech recognition, and unified visual dubbing—SyncLipMAE achieves state-of-the-art performance, validating the effectiveness of this pretraining strategy.

REFERENCES

- Relja Arandjelovic and Andrew Zisserman. Look, listen and learn. In *Proceedings of the IEEE international conference on computer vision*, pp. 609–617, 2017.
- Zhixi Cai, Shreya Ghosh, Kalin Stefanov, Abhinav Dhall, Jianfei Cai, Hamid Rezatofighi, Reza Haffari, and Munawar Hayat. Marlin: Masked autoencoder for facial video representation learning. In *Proceedings of the IEEE/CVF conference on computer vision and pattern recognition*, pp. 1493–1504, 2023.
- Joon Son Chung and Andrew Zisserman. Out of time: automated lip sync in the wild. In *Asian conference on computer vision*, pp. 251–263. Springer, 2016.
- Jiahao Cui, Hui Li, Yun Zhan, Hanlin Shang, Kaihui Cheng, Yuqi Ma, Shan Mu, Hang Zhou, Jingdong Wang, and Siyu Zhu. Hallo3: Highly dynamic and realistic portrait image animation with video diffusion transformer. In *Proceedings of the Computer Vision and Pattern Recognition Conference*, pp. 21086–21095, 2025.
- Kaiming He, Xinlei Chen, Saining Xie, Yanghao Li, Piotr Dollár, and Ross Girshick. Masked autoencoders are scalable vision learners. In *Proceedings of the IEEE/CVF conference on computer vision and pattern recognition*, pp. 16000–16009, 2022.
- Martin Heusel, Hubert Ramsauer, Thomas Unterthiner, Bernhard Nessler, and Sepp Hochreiter. Gans trained by a two time-scale update rule converge to a local nash equilibrium. *Advances in neural information processing systems*, 30, 2017.
- Zeyinzi Jiang, Zhen Han, Chaojie Mao, Jingfeng Zhang, Yulin Pan, and Yu Liu. Vace: All-in-one video creation and editing. *arXiv preprint arXiv:2503.07598*, 2025.
- Venkatesh S Kadandale, Juan F Montesinos, and Gloria Haro. Vocalist: An audio-visual synchronisation model for lips and voices. *arXiv preprint arXiv:2204.02090*, 2022.
- Bruno Korbar, Du Tran, and Lorenzo Torresani. Scsampler: Sampling salient clips from video for efficient action recognition. In *Proceedings of the IEEE/CVF International Conference on Computer Vision*, pp. 6232–6242, 2019.
- Chunyu Li, Chao Zhang, Weikai Xu, Jingyu Lin, Jinghui Xie, Weiguo Feng, Bingyue Peng, Cunjian Chen, and Weiwei Xing. Latentsync: Taming audio-conditioned latent diffusion models for lip sync with syncnet supervision. *arXiv preprint arXiv:2412.09262*, 2024.
- Steven R Livingstone and Frank A Russo. The ryerson audio-visual database of emotional speech and song (ravdess): A dynamic, multimodal set of facial and vocal expressions in north american english. *PloS one*, 13(5):e0196391, 2018.
- Pingchuan Ma, Alexandros Haliassos, Adriana Fernandez-Lopez, Honglie Chen, Stavros Petridis, and Maja Pantic. Auto-avsr: Audio-visual speech recognition with automatic labels. In *ICASSP 2023-2023 IEEE International Conference on Acoustics, Speech and Signal Processing (ICASSP)*, pp. 1–5. IEEE, 2023.
- Pedro Morgado, Yi Li, and Nuno Nvasconcelos. Learning representations from audio-visual spatial alignment. *Advances in Neural Information Processing Systems*, 33:4733–4744, 2020.
- William Peebles and Saining Xie. Scalable diffusion models with transformers. In *Proceedings of the IEEE/CVF international conference on computer vision*, pp. 4195–4205, 2023.
- KR Prajwal, Rudrabha Mukhopadhyay, Vinay P Nambodiri, and CV Jawahar. A lip sync expert is all you need for speech to lip generation in the wild. In *Proceedings of the 28th ACM international conference on multimedia*, pp. 484–492, 2020.

- Alec Radford, Jong Wook Kim, Chris Hallacy, Aditya Ramesh, Gabriel Goh, Sandhini Agarwal, Girish Sastry, Amanda Askell, Pamela Mishkin, Jack Clark, et al. Learning transferable visual models from natural language supervision. In *International conference on machine learning*, pp. 8748–8763. PmLR, 2021.
- Bowen Shi, Wei-Ning Hsu, Kushal Lakhota, and Abdelrahman Mohamed. Learning audio-visual speech representation by masked multimodal cluster prediction. In *International Conference on Learning Representations*, 2022.
- Licai Sun, Zheng Lian, Bin Liu, and Jianhua Tao. Mae-dfer: Efficient masked autoencoder for self-supervised dynamic facial expression recognition. In *Proceedings of the 31st ACM International Conference on Multimedia*, pp. 6110–6121, 2023.
- Zhan Tong, Yibing Song, Jue Wang, and Limin Wang. Videomae: Masked autoencoders are data-efficient learners for self-supervised video pre-training. *Advances in neural information processing systems*, 35:10078–10093, 2022.
- Thomas Unterthiner, Sjoerd Van Steenkiste, Karol Kurach, Raphael Marinier, Marcin Michalski, and Sylvain Gelly. Towards accurate generative models of video: A new metric & challenges. *arXiv preprint arXiv:1812.01717*, 2018.
- Team Wan, Ang Wang, Baole Ai, Bin Wen, Chaojie Mao, Chen-Wei Xie, Di Chen, Feiwu Yu, Haiming Zhao, Jianxiao Yang, et al. Wan: Open and advanced large-scale video generative models. *arXiv preprint arXiv:2503.20314*, 2025.
- Kaisiyuan Wang, Qianyi Wu, Linsen Song, Zhuoqian Yang, Wayne Wu, Chen Qian, Ran He, Yu Qiao, and Chen Change Loy. Mead: A large-scale audio-visual dataset for emotional talking-face generation. In *European conference on computer vision*, pp. 700–717. Springer, 2020.
- Liangbin Xie, Xintao Wang, Honglun Zhang, Chao Dong, and Ying Shan. Vfhq: A high-quality dataset and benchmark for video face super-resolution. In *Proceedings of the IEEE/CVF Conference on Computer Vision and Pattern Recognition*, pp. 657–666, 2022.
- Jianhui Yu, Hao Zhu, Liming Jiang, Chen Change Loy, Weidong Cai, and Wayne Wu. Celebv-text: A large-scale facial text-video dataset. In *Proceedings of the IEEE/CVF Conference on Computer Vision and Pattern Recognition*, pp. 14805–14814, 2023.
- Yue Zhang, Zhizhou Zhong, Minhao Liu, Zhaokang Chen, Bin Wu, Yubin Zeng, Chao Zhan, Yingjie He, Junxin Huang, and Wenjiang Zhou. Musetalk: Real-time high-fidelity video dubbing via spatio-temporal sampling. *arXiv preprint arXiv:2410.10122*, 2024.
- Zhimeng Zhang, Lincheng Li, Yu Ding, and Changjie Fan. Flow-guided one-shot talking face generation with a high-resolution audio-visual dataset. In *Proceedings of the IEEE/CVF conference on computer vision and pattern recognition*, pp. 3661–3670, 2021.
- Hao Zhu, Wayne Wu, Wentao Zhu, Liming Jiang, Siwei Tang, Li Zhang, Ziwei Liu, and Chen Change Loy. Celebv-hq: A large-scale video facial attributes dataset. In *European conference on computer vision*, pp. 650–667. Springer, 2022.

Table 6: Ablations on **Hallo3** (audio–visual stream synchronization). Higher is better for Acc and R-Precision; lower is better for Offset.

Variant	K = 1		K = 5		K = 15		R-precision (32)		
	Acc \uparrow (%)	Offset \downarrow	Acc \uparrow (%)	Offset \downarrow	Acc \uparrow (%)	Offset \downarrow	Top1 \uparrow	Top2 \uparrow	Top3 \uparrow
<i>(A) Two-Bypass Face-Aware Masking</i>									
A1 Uniform-only (single view)	9.34	7.18	12.68	6.22	18.57	5.36	2.83	5.14	7.92
A2 Face-aware-only (single view)	45.63	3.45	61.07	2.37	75.88	1.27	33.45	52.81	66.19
A3 Two-bypass w/o photometric	49.62	3.02	65.91	2.03	79.87	1.05	37.54	57.89	70.86
<i>(B) Audio Feature Adaptation</i>									
B1 Last-layer only	42.68	3.62	58.34	2.51	73.45	1.36	30.92	49.87	63.11
<i>(C) Decoder Cross-Attention</i>									
C1 No cross-attention	48.27	3.10	64.31	2.09	78.44	1.09	36.21	56.48	69.32
Ours	52.53	2.66	68.41	1.73	82.27	0.93	40.18	61.48	73.49

Table 7: Audio–visual stream synchronization on **CelebV-HQ**. Higher is better for Acc/R-precision; lower is better for Offset.

Smooth window Method	K=1		K=5		K=15		R-precision (32)		
	Acc \uparrow (%)	Offset \downarrow	Acc \uparrow (%)	Offset \downarrow	Acc \uparrow (%)	Offset \downarrow	Top1 \uparrow	Top2 \uparrow	Top3 \uparrow
SyncNet	20.26	6.14	24.50	5.67	32.07	4.99	8.08	14.90	20.91
VocalIST – LRS2	17.42	6.60	20.46	6.38	25.96	5.89	5.98	11.59	16.45
StableSyncNet	32.95	4.66	34.35	4.62	38.04	4.44	21.26	33.20	40.69
Ours	32.63	4.83	40.96	4.41	52.91	3.56	28.47	44.19	54.32

A ABLATION STUDIES

Two-Bypass Face-Aware Masking. We evaluate four variants on **Hallo3** using the same A/V synchronisation protocol as the main results (Acc $_{\pm K}$, Offset, R-precision; see Tab 6). *A1 (Uniform-only)* severely underperforms: heavy uniform masking hides the lip region, the contrastive loss scarcely decreases, and all sync metrics degrade markedly. *A2 (Face-aware-only)* trains the contrastive objective but yields weaker reconstruction guidance, producing normal yet inferior sync scores. *A3 (Two-bypass w/o photometric)* restores learning stability but, without motion-view photometric jitter, motion tokens leak appearance; alignment improves over A2 but remains below the best. *A4 (Two-bypass + photometric, ours)* is strongest across all metrics, confirming that a uniform view for reconstruction context plus a face-preserving view—with photometric perturbations—for prompt tokens best supports token-level A/V alignment.

Audio Feature Adaptation. We compare *B1 (Last-layer only)* versus *B2 (Concat→Adapter, ours)*. B1 is consistently worse than A2 and B2: using only the wav2vec 2.0 final layer emphasizes semantic content and attenuates fine-grained timing, leading to lower Acc $_{\pm K}$, higher Offset, and reduced R-precision. B2 concatenates all hidden layers and adapts them to the visual width, yielding the highest synchronisation scores among the audio variants.

Decoder Cross-Attention. We ablate *C1 (No cross-attention)* against *C2 (CA to id+amb+c_l, ours)*. In C1, when prompt tokens are simply concatenated with patch tokens before self-attention, the decoder tends to ignore them, slightly underperforming A3. C2 explicitly cross-attends to identity,

Table 8: Audio–visual stream synchronization on **CelebV-Text**. Higher is better for Acc/R-precision; lower is better for Offset.

Smooth window Method	K=1		K=5		K=15		R-precision (32)		
	Acc \uparrow (%)	Offset \downarrow	Acc \uparrow (%)	Offset \downarrow	Acc \uparrow (%)	Offset \downarrow	Top1 \uparrow	Top2 \uparrow	Top3 \uparrow
SyncNet	18.80	6.10	22.73	5.40	28.85	4.56	8.89	15.03	20.54
VocalIST – LRS2	22.05	5.87	25.96	5.39	32.27	4.64	11.08	17.66	23.04
StableSyncNet	34.42	3.93	35.51	3.88	37.58	3.76	27.02	37.25	43.35
Ours	34.95	5.10	46.46	4.44	60.60	3.51	25.80	39.02	47.99

Table 9: Audio–visual stream synchronization on **MEAD**. Higher is better for Acc/R-precision; lower is better for Offset.

Smooth window	K=1		K=5		K=15		R-precision (32)		
	Acc ↑ (%)	Offset ↓	Acc ↑ (%)	Offset ↓	Acc ↑ (%)	Offset ↓	Top1 ↑	Top2 ↑	Top3 ↑
SyncNet	39.39	4.01	50.03	2.97	61.18	1.85	20.74	32.29	40.01
VocaliST – LRS2	35.02	4.59	43.81	3.64	55.60	2.50	15.69	26.03	33.61
StableSyncNet	57.51	2.05	60.36	1.85	64.25	1.57	37.20	54.19	62.83
Ours	45.90	2.77	56.20	2.04	69.76	1.30	38.63	60.94	74.36

Table 10: Audio–visual stream synchronization on **RAVDSS**. Higher is better for Acc/R-precision; lower is better for Offset.

Smooth window	K=1		K=5		K=15		R-precision (32)		
	Acc ↑ (%)	Offset ↓	Acc ↑ (%)	Offset ↓	Acc ↑ (%)	Offset ↓	Top1 ↑	Top2 ↑	Top3 ↑
SyncNet	20.54	9.38	26.76	8.79	38.52	7.54	14.47	22.69	28.48
VocaliST – LRS2	22.12	8.93	27.97	8.33	39.96	7.15	14.94	23.46	29.21
StableSyncNet	42.69	6.91	46.06	6.62	53.79	5.97	34.51	46.21	51.28
Ours	47.94	3.09	61.03	2.37	79.03	1.23	39.97	62.90	76.26

ambient, and the conditioning token $c_t \in \{\mathbf{z}_t^{\text{voc}}, \mathbf{A}_t\}$, which improves A/V alignment and yields the best overall sync metrics.

B MORE RESULTS

Audio–visual stream synchronization. We additionally evaluate SyncLipMAE on **CelebV-HQ**, **CelebV-Text**, **RAVDSS**, and **MEAD**, and report these results in the Appendix. We do so because these corpora contain substantial non-speech or highly repeated content that can confound lag metrics and retrieval: CelebV-HQ and CelebV-Text are broad, face-centric video sets with attributes beyond active speech (appearance, actions, emotions, diverse in-the-wild clips), so many segments are not strictly speaking-focused; RAVDESS and MEAD are acted emotion datasets captured in controlled settings, with RAVDESS using only two fixed sentences across many takes (plus sung versions), leading to heavy lexical repetition.

Experimental analysis. Across all four datasets, SyncLipMAE shows consistent gains in both temporal alignment (higher $\text{Acc}_{\pm K}$, lower Offset) and cross-modal retrieval (higher R-precision@k). Improvements are most pronounced on the controlled emotion corpora (MEAD/RAVDSS), where reduced acoustic and visual variability amplifies the benefit of our token-level alignment; on the in-the-wild CelebV-HQ/CelebV-Text, gains remain steady despite non-speech spans and repeated content. Notably, all results are achieved with single-frame visual conditioning ($n=1$), indicating strong per-frame audio–visual correspondence without reliance on long temporal windows.

C LIMITATION

While SyncLipMAE achieves strong results across four disparate tasks, several limitations remain. (1) Model size and deployability. Compared with classic synchronisation backbones such as SyncNet—which is lightweight enough to be used directly as an evaluation head or even as a discriminator/loss in generation systems like Wav2Lip—SyncLipMAE is substantially heavier, making “drop-in loss” usage during training less practical and raising compute and memory costs for deployment.

(2) Scope of applicability. Although SyncLipMAE aligns audio and visual tokens well for lip-sync, expression/action understanding, and VSR, it is not a universal solution for all audio–face problems. For example, when we followed a speech-to-3DMM pipeline (in the spirit of audio-driven 3D talking-head methods) and drove 3D parameters using SyncLipMAE’s audio branch, the results were generally underwhelming—suggesting that additional geometry-aware supervision or models tailored to 3D priors are needed. (3) Factorization remains preliminary. Our decomposition into identity, vocal motion, and ambient motion is a first step; most of our downstream usage centers on

the vocal-motion token. Systematically exploiting the other two factors (e.g., identity-aware editing, ambient-motion analysis/transfer) and strengthening disentanglement are promising directions for future work.